On the Effects of Wind Tunnel Floor Tangential Blowing on the Aerodynamic Forces of Passenger Vehicles

Downloaded from: https://research.chalmers.se, 2026-04-04 04:59 UTC

Citation for the original published paper (version of record):
Ljungskog, E., Sebben, S., Broniewicz, A. et al (2017). On the Effects of Wind Tunnel Floor Tangential Blowing on the Aerodynamic Forces of Passenger
Vehicles. SAE International Journal of Passenger Cars - Mechanical Systems, 10(2): 591-599.
http://dx.doi.org/10.4271/2017-01-1518

N.B. When citing this work, cite the original published paper.

research.chalmers.se offers the possibility of retrieving research publications produced at Chalmers University of Technology. It covers all kind of research output: articles, dissertations, conference papers, reports etc. since 2004. research.chalmers.se is administrated and maintained by Chalmers Library

(article starts on next page)

17SS-0254

On the Effects of Wind Tunnel Floor Tangential Blowing on the Aerodynamic Forces of Passenger Vehicles

Emil Ljungskog, Simone Sebben
Chalmers University of Technology

Alexander Broniewicz, Christoffer Landström
Volvo Cars

Abstract

Many aerodynamic wind tunnels used for testing of ground vehicles have advanced ground simulation systems to account for the relative motion between the ground and the vehicle. One commonly used approach for ground simulation is a five belt system, where moving belts are used, often in conjunction with distributed suction and tangential blowing that reduces the displacement thickness of the boundary layer along the wind tunnel floor. This paper investigates the effects from aft-belt tangential blowing in the Volvo Cars Aerodynamic wind tunnel. First the uniformity of the boundary layer thickness downstream of the blowing slots is examined in the empty tunnel. This is followed by investigations of how the measured performance of different vehicle types in several configurations, typically tested in routine aerodynamic development work, depends on whether the tangential blowing system is active or not. Numerical simulations are also used to explain the flow field origin of the force differences measured in the wind tunnel. Results show that even though the displacement thickness behind the blowers varies along the width of the blowing slots, it is significantly reduced compared to the case of no blowing; furthermore, it is also shown that deactivating the blowing altogether has an effect not only on the absolute forces but also on the deltas measured between different configurations, and that this phenomenon is more prominent if the vehicle has a larger base area.

Introduction

In recent years, sustainability and reduced environmental impact has become one of the main focus areas in automotive research and development. One aspect of the environmental friendliness of a vehicle is its fuel consumption, which is influenced by a number of attributes, of which aerodynamics is an important one.

The classical tool for aerodynamic evaluation and optimization is the wind tunnel. In order to properly simulate the correct relative movement between a vehicle and the ground, an automotive wind tunnel should be equipped with a ground simulation system. There are three common methods used in such systems; moving belts, distributed suction, and tangential blowing. These methods are often used in conjunction, for example, in a five belt system. The layout and operation of the ground simulation has a significant impact on the aerodynamic forces measured on the vehicle, as has been well pointed out in the literature. For example, Wiedemann [1] showed that not only the absolute values of drag but also the differences between configurations are affected by the ground simulation technique employed in the tunnel. Furthermore, it was showed that the effects from the ground simulation are not only present for geometry changes to the underbody close to the ground, but also to alterations of the top hat such as adding a rear wing.

Previous studies of tangential blowing in automotive wind tunnels mainly treated tangential blowing as an alternative for distributed suction or a moving belt [2–4]. The studies concluded that tangential blowing is a good alternative to distributed suction due to a lower impact on the pitch angle of the flow. However, a major shortcoming is that it has to be calibrated to give an optimal displacement thickness at a single longitudinal position downstream of the blowing slot, often at the position of the front wheels. An alternative application of tangential blowing is to use it upstream of a moving belt to refill the momentum deficit of the boundary layer created upstream of the belt, as investigated by Cogotti [5] and Potthoff [6].

A less commonly studied tangential blowing configuration is to extend the apparent length of a moving belt by applying the blowing just downstream of the belt. The present paper investigates such a setup in the Volvo Cars aerodynamic wind tunnel. First, the boundary layer displacement thickness downstream of the tangential blowers is examined for the empty tunnel, followed by a study of the impact from this tangential blowing arrangement on the force deltas measured between aerodynamic configurations on two production cars. The two configurations showing the largest sensitivity to blowing are then investigated using CFD and the flow field differences leading to the force changes are discussed.

Methodology

Wind tunnel

All physical tests presented in this paper were performed in the Volvo Cars Aerodynamic wind tunnel in Gothenburg, Sweden. The tunnel is a slotted wall, closed return (Göttingen) wind tunnel with a test section cross-sectional area of $27.06\,\mathrm{m}^2$. It was built in the mid 1980s to be fully operational 1986 and was upgraded with a more powerful fan and a five belt boundary layer control system (BLCS) in 2006, as described by Sternéus et al. [7]. The full BLCS consists of a basic suction scoop, two distributed suction zones, five moving belts and five tangential blowers, as outlined in Figure 1.

Four out of the five tangential blowers are mounted behind the wheel drive units (WDU), and one behind the centre belt. Each WDU blower unit consists of a 600 mm wide and 0.6 mm tall blowing slot at the exit of a settling chamber. The centre belt blower is constructed in a similar way, but with a blowing slot that is 1000 mm wide and 1 mm tall. All five blowers are connected to the same compressor, with a valve before each blower unit to allow for tuning of the pressure in each individual settling chamber and thereby the blowing speed and momentum injected into the boundary layer.

The tangential blowers are calibrated to minimize the displacement thickness 800 mm downstream of each blower for every freestream velocity. This location was chosen during the commissioning of the wind tunnel as a reasonable distance for the blower to compensate for the stationary ground between the wheels, as well as allowing the main

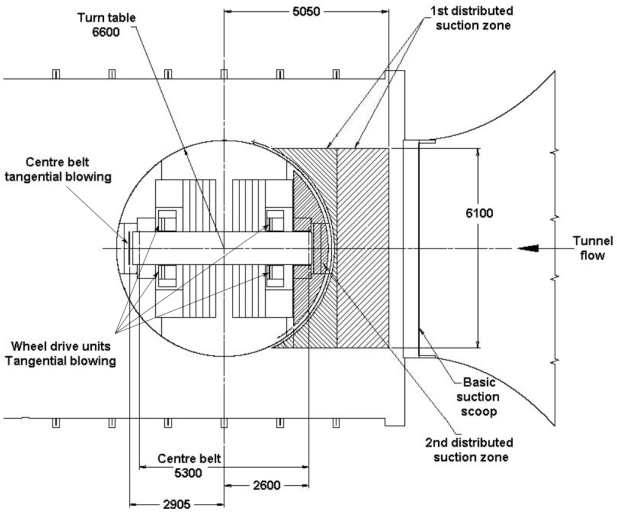

Figure 1: Wind tunnel floor layout with boundary layer control systems. Adapted from [7].

Table 1: Force coefficient repeatability within a test.

Force	Coefficient	Repeatability
Drag	C_D	±0.001
Front lift	C_{LF}	±0.001
Rear lift	C_{LR}	±0.005

part of the velocity overshoot behind the blower to flatten out. The freestream velocity dependency is achieved by slaving the fan speed of the compressor driving the blowers to the freestream wind speed.

As for all measurements, wind tunnel data has a level of uncertainty. In the case of the force measurements in the wind tunnel considered here, this level is quantified by the repeatability of the force coefficients between two tests and within a test, the difference being whether or not the car is removed and reinstalled between the measurements. For the present work, the car is not removed between measurements, which is why the within test repeatability given in Table 1 is applicable.

Boundary layer thickness measurements

In order to measure the boundary layer thickness behind the tangential blowers in the empty tunnel, a rake of total pressure probes was mounted on the wind tunnel traversing gear and positioned such that the first probe was located 2 mm above the tunnel floor. The rake consisting of 22 probes over a total height of 109 mm can be seen in Figure 2. The longitudinal position of the rake was fixed 800 mm downstream of the blower while the rake was traversed throughout the width of the slot at a sweep speed of 20 mm/s with a sampling frequency of 20 Hz and 5 frames per sample, thus resulting in roughly one measurement per millimeter.

The thickness of the boundary layer was quantified using the displacement thickness δ^*, defined as

$$\delta^* = \int_0^\infty \left(1 - \frac{u(z)}{u_\infty}\right) \mathrm{d}z,$$

with z directed upwards from the floor and the local velocity $u(z)$ calculated as

$$u(z) = \sqrt{\frac{2q(z)}{\rho_s}}.$$

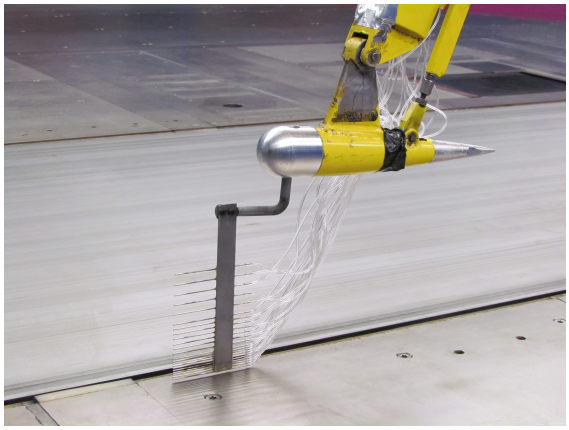

Figure 2: Boundary layer rake mounted on the traversing gear.

The dynamic pressure $q(z)$ was found from the total pressure measurements using the compressible flow relation

$$q(z) = \frac{\gamma}{\gamma+1} P_s \left(\left(\frac{P_t(z) - P_s}{P_s} + 1 \right)^{\frac{\gamma-1}{\gamma}} - 1 \right),$$

where $\gamma = 1.4$ is the ratio of specific heats for air, P_s the test section static pressure and $P_t(z)$ the total pressure measured by the probe rake.

Tangential blowing influence on aerodynamic force deltas

The influence from tangential blowing on aerodynamic force deltas for a number of common aerodynamic configurations was investigated using two similar cars with different rear end shapes, namely a notchback Volvo S60 and a squareback Volvo V60. Apart from the shape difference at the rear, the two cars were identical with respect to powertrain, wheels and styling levels.

Physical experiments in the wind tunnel were used to quantify sensitivities and interactions, while numerical investigations were used to gain insight into the flow field changes potentially causing the phenomena observed in the physical tests.

Experimental setup

For each car, seven factors were tested using a design of experiments approach with a two-level 2^{7-3}_{IV} fractional factorial design [8] in order to be able to quantify both main effects and two factor interactions. The tested factors can be seen in Table 2, which also shows the two levels for each factor used in the experimental design. A selection of the factors is shown mounted on the cars in Figure 3. All factors except the cooling flow blanking, bootlid spoiler and aero blades were screwed in place, ensuring reliable positioning between the runs. The cooling blanking, spoiler and blades were fastened using tape, with great care taken to accurately fix them in the same position for each run in order to minimize any variability. The seven factors were chosen since they were expected to influence the aerodynamic forces by changing the mass flow under the car and/or the properties of the base wake. For the squareback, the bootlid spoiler was replaced by aero blades. The baseline configuration was taken as the configuration that was expected to have the highest drag value, which meant open cooling, high ride height and no aerodynamic devices mounted.

The experimental design was chosen to fulfill a requirement on the

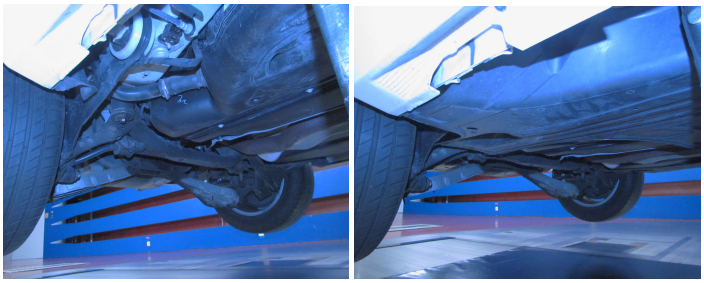

(a) Underfloor panels off (b) Underfloor panels on

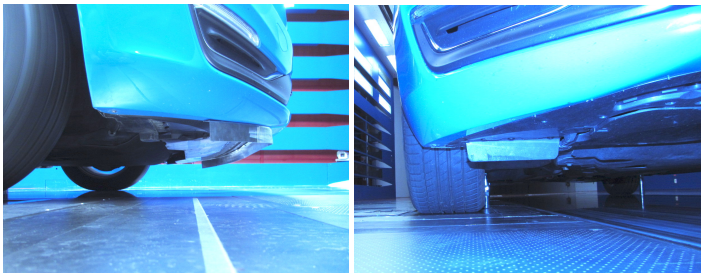

(c) Air dam (d) Front wheel deflector

(e) Aero blades (squareback only) (f) Bootlid spoiler (notchback only)

Figure 3: The tested configurations.

Table 2: Investigated factors and their levels in the experimental design.

Factor	Encoding	Low level	High level
Ride height	A	−15 mm	Reference
Bootlid spoiler/aero blades	B	Off	On
Air dam	C	Off	On
Underfloor panels	D	Off	On
Front wheel deflectors	E	Off	On
Covered rims	F	Off	On
Cooling flow	G	Closed	Open

Table 3: Confounding structure for the two factor interactions in the employed 2^{7-3}_{IV} fractional factorial design.

Interaction	Confounding structure
AB	AB + CE + FG
AC	AC + BE + DG
AD	AD + CG + EF
AE	AE + BC + DF
AF	AF + BG + DE
AG	AG + BF + CD
BD	BD + CF + EG

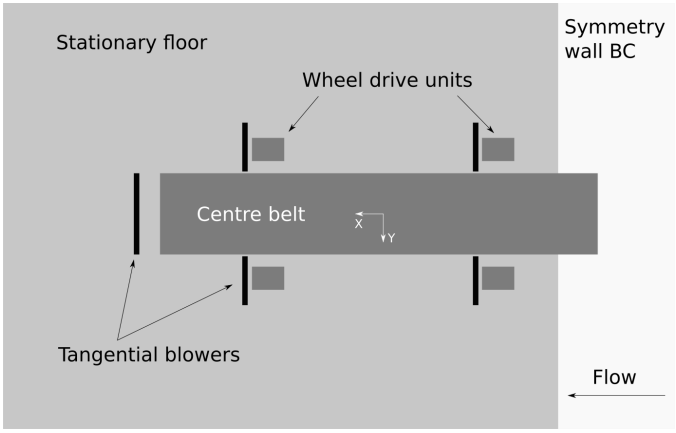

Figure 4: Moving ground system as modeled in CFD.

maximum number of runs estimated to fit into the allocated wind tunnel time. However, since the design is of resolution four, two factor interactions are confounded with other two factor interactions and can thus not be uniquely estimated [8]. The confounding pattern for the two factor interactions of the employed design can be seen in Table 3. Consider for example the AF interaction, with the confounding structure AF + BG + DE. This means that we cannot estimate AF itself, but just the sum of the interactions between ride height and covered rims (AF), bootlid spoiler/aero blades and cooling flow (BG), and underfloor panels and front wheel deflectors (DE). In order to avoid this two factor confounding, a design with a resolution of at least five would need to be employed, which for this case would lead to an unacceptable fourfold increase of the number of performed test runs from 16 to 64.

For each run in the experimental design, the aerodynamic forces on the car were measured both with the tangential blowing on and off. Each force coefficient was then compared to the baseline with the same blowing setting. In this way, each run resulted in two delta values for each force coefficient; one for tangential blowing on, and one for off. The response variable considered is the delta-of-deltas, i.e. the difference between those two deltas, which means that if the delta measurement is robust with respect to the tangential blowing, the response will be zero.

Numerical setup

The simulations were performed in STAR-CCM+ using the SST $k-\omega$ Improved Delayed Detached Eddy Simulation (IDDES) approach. For each configuration, the flow was allowed to develop before averaging for 3 seconds. The same freestream velocity of 140 km/h was used in the simulations as in the physical tests.

In the numerical simulations, the full geometry of the test section in the physical wind tunnel was not included. However, the five moving belts were included as a moving wall boundary condition, while the floor upstream of the belts was modeled as a symmetry wall to ensure that there was no incoming boundary layer to the belts. To include the geometry of the tangential blower systems, and especially the thin blowing slots, would require a prohibitively fine mesh resolution. Instead, the approach introduced by Olander [9], where the tangential blowing is introduced on a patch of the floor as a mass flow inlet with an injection direction that is near tangential to the wall, was used. The layout of the moving ground system, as modeled in CFD, can be seen in Figure 4.

The injected mass flow for each WDU blower was calibrated to match the displacement thickness of the boundary layer measurements, while the centre belt mass flow was adjusted so that the displacement thickness vanished 800 mm downstream of the blowing slot. Both these calibrations were done without a car in place.

Wheel rotation was modeled using a moving wall boundary condition

on the slick tyres, and MRF zones in between the spokes of the rims. The radiators in the cooling package were modeled using porous media, while the wind-milling rotation of the cooling fans was simulated using MRF zones. For the mesh, a total of 12 prism layers with a first layer thickness of 0.0075 – 0.025 mm depending on location, and total thickness of 8 mm, were used on the upper body of the car to ensure that the boundary layer was resolved with $y^+ < 1$, while two 0.5 mm thick prism layers were built on the underbody and in the engine bay. On the stationary ground, 8 prism layers with a near wall thickness of 1 mm and a total height of 16 mm were used to account for the boundary layer buildup.

Results and discussion

Boundary layer thickness uniformity

Figure 5 shows the displacement thickness across the tangential blower slot behind each wheel drive unit for the empty tunnel with all boundary layer control systems active. Measurements for the centre belt blower are not available. The blowing slot spans the region $520\,\text{mm} \leq |y| \leq 1120\,\text{mm}$. As expected, there is a difference in δ^* between the front and the rear since the boundary layer will grow along the floor behind the front unit. This is especially clear when comparing the regions unaffected by the tangential blowing, at $|y| \gtrsim 1150\,\text{mm}$, where the rear measurements exhibit a considerably thicker boundary layer.

Apart from the differences between front and rear there is also an asymmetry between the left and right sides, especially close to the centre belt. This is particularly clear for the front blowers in Figures 5a and 5b. The reasons why the largest differences occur in this area cannot be determined from the performed measurements, but one possibility is that they are caused by parts of a nylon strip that was originally acting as a spacing between the centre belt and the fixed ground, but has gradually fallen off. An example of such residue can be seen in the gap between the stationary floor and the centre belt, just upstream of the probe rake in Figure 2.

It can also be seen in Figure 5 that the boundary layer thickens close to the centre belt. Again, the measurements do not provide a basis upon which to build any firm conclusions about the cause of this phenomenon, but it is hypothesized that it is caused by a three dimensional swirl originating from the interface between the centre belt and the stationary floor. Such an effect would also explain the bumps in displacement thickness seen behind the edges of the WDU belts for the front positions.

Assuming that the boundary layer thickness in the region not affected by the blowing is the same thickness the boundary layer would have if the tangential blowing were turned off, it can be concluded that the tangential blowing is having a considerable effect on reducing the displacement thickness. It can even be noted that $\delta^* < 0$ in some parts behind the WDU:s, meaning that the boundary layer has a momentum excess due to a too high blowing speed. Furthermore, the displacement thickness increases with the freestream velocity of the tunnel, which is particularly clear for the 200 km/h case where the pressures in the settling chambers are near the maximum capacity of the system.

Verification of blower modeling in CFD

A comparison between physical measurements and CFD of the displacement thickness 800 mm behind the front left tangential blower for a freestream velocity of 140 km/h can be seen in Figure 6. It can be noted that the overall behavior of the boundary layer thickness is well captured, except for the bumps believed to be caused by the upstream WDU belt, although some effect of the WDU can be seen as a slightly

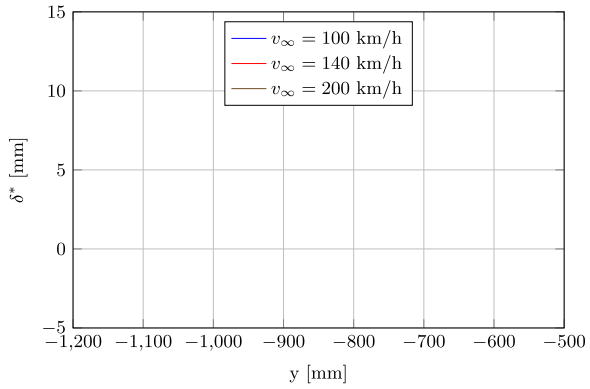

(a) Front left

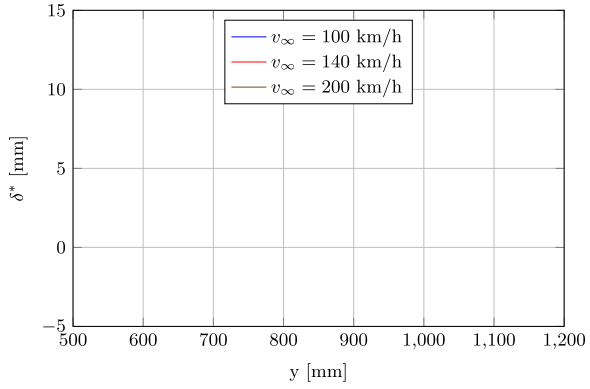

(b) Front right

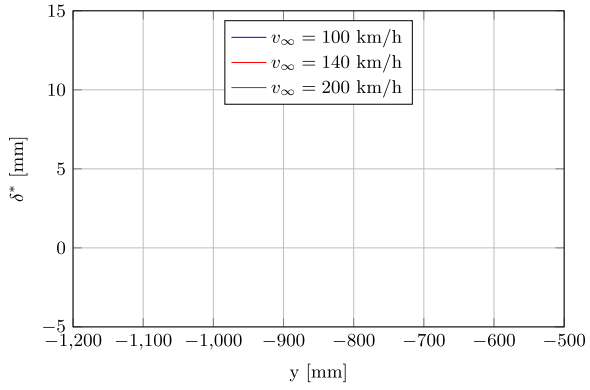

(c) Rear left

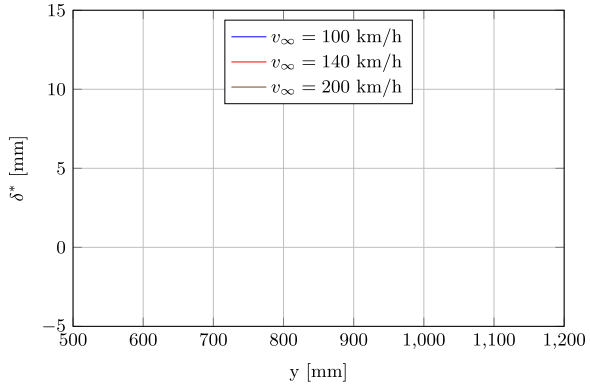

(d) Rear right

Figure 5: Displacement thickness across the tangential blower slot 800 mm behind each wheel drive unit blower with all boundary layer systems active. Shaded areas represent the location of the upstream wheel drive units.

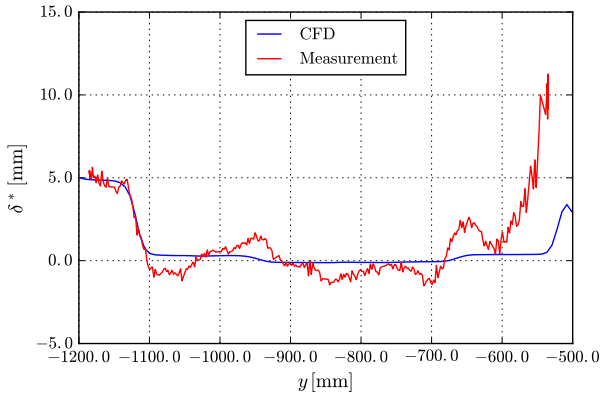

Figure 6: Comparison of displacement thickness 800 mm downstream of the front left blower in the empty tunnel for the freestream velocity 140 km/h.

lower displacement thickness behind it. Furthermore, since the floor geometry in the CFD model is completely flat, the thickening of the boundary layer seen close to the centre belt in the physical tunnel is not fully captured in the numerical simulations.

The fact that the boundary layer cannot be perfectly reproduced in the CFD simulations without a car increases the uncertainty when comparisons are made to absolute force values from the wind tunnel. This might also be a contributing factor to the difference seen in the magnitude of the delta-of-deltas discussed below. It should also be noted that even though the main influence of the blowing on the displacement thickness is captured, it is likely that the exact velocity profile of the jet is not. However, it is believed that the displacement thickness is a good measure of the global impact of the tangential blowing.

Effects on aerodynamic force deltas

Figures 7 and 8 show the effect on measured delta and delta-of-deltas values from tangential blowing for each single factor and two factor interaction. Significance of the delta-of-deltas is judged by the wind tunnel repeatability given in Table 1 and indicated by horizontal lines in the figures. Using a normal plot gives the same significant effects, why the wind tunnel repeatability is deemed to be a sufficient significance measure.

Comparing Figures 7 and 8, it can be seen that the influence on the measured deltas-of-deltas from the blowing is considerably more prominent for the squareback than for the notchback, especially for drag. The effects on front lift are similar between the two vehicles, while all effects for rear lift falls within the test uncertainty. The larger effects on the squareback indicate that the main influence from the tangential blowing is acting on the rear of the car, where the only geometrical differences between the cars occur.

Focusing on the drag coefficient, it can be seen that for the notchback only the air dam (C) and the cooling flow (G) have a significant sensitivity to the tangential blowing. This is in sharp contrast to the squareback, where not only the number of significant deltas-of-deltas is larger, but their magnitudes are also greatly increased. It is clear that the most sensitive of the tested aerodynamic configurations is the cooling blanking (G), for which the $\Delta\Delta C_D$ is 8 drag counts, or 47% of the closed cooling ΔC_D. Such differences are large enough to influence decisions on whether a certain configuration should be included in production or not. Furthermore, deltas-of-deltas for ride height (A), air dam (C) and underfloor panels (D) show a significant sensitivity for the squareback, as well as the interactions AB, AC and BD. Although significant in the statistical sense, the interactions are small compared to the main effects.

It can be noted that the trend in ΔC_D relative to the baseline is not changed by the tangential blowing for any configuration except for the air dam (C), for which the drag drops slightly when the blowing is turned off, but stays unchanged when the blowing is on. This holds for both the notchback and the squareback.

Regarding front lift, it can be seen that both the air dam (C) and covered rims (F) are measurably sensitive to tangential blowing for both cars. Both cars also have one significant interaction each; AD for the notchback and AB for the squareback. However, it should be noted that the sensitivity of the deltas-of-deltas for front lift are very small in comparison to the deltas compared to baseline.

Flow field investigations

For the wind tunnel results, the drag delta was the difference between for example closed cooling and baseline for each blower mode as

$$\Delta C_{D_{\text{closed, TB on}}} = C_{D_{\text{closed, TB on}}} - C_{D_{\text{baseline, TB on}}}$$
$$\Delta C_{D_{\text{closed, TB off}}} = C_{D_{\text{closed, TB off}}} - C_{D_{\text{baseline, TB off}}}.$$

Now, the considered drag delta for the closed cooling case is instead defined as

$$\Delta C_{D_{\text{closed}}} = C_{D_{\text{closed, TB on}}} - C_{D_{\text{closed, TB off}}}.$$

The reason for this change of view is to do comparisons between more similar cases in order to make it easier to identify differences.

The accumulated drag difference along the length of the car between tangential blowing on and off for both open and closed cooling can be seen in Figure 9. It can be noted that the trend for $\Delta\Delta C_D$ seen in the wind tunnel is also captured in CFD, even though the magnitude is smaller. From the accumulated drag in Figure 9, it can be seen that $\Delta\Delta C_D \approx 0.002$ in CFD, and effect G in Figure 8a shows that $\Delta\Delta C_D = 0.008$ in the tunnel. Furthermore, Figure 9 shows that the main influence of the tangential blowing acts in the rear of the car, mainly around the rear wheels and on the base. Especially on the base of the car, the trend shifts between open and closed cooling, which is clear when looking at the difference in pressure on the base in Figure 10. It can be seen that the tangential blowing lowers the pressure on the upper half of the right hand side of the base for open cooling, while the opposite is true when the cooling flow is closed. In fact, a comparatively large increase in pressure on the upper half of the base can be seen for the blowing on condition with closed cooling but not with open cooling. The fact that this main difference in impact on the base pressure is acting on the upper part of the base could explain why the effect seen for the notchback is less prominent.

Considering the pressure coefficient deltas on the centre plane of the base wake in Figure 11, it can be seen that the blowing lowers the pressure upstream of the centre belt blower for both open and closed cooling and increases the pressure downstream due to the energy injection. However, in the closed cooling case, a slight pressure increase can be seen near the base, corresponding to the higher base pressure seen in Figure 10. The main reason for this behavior has not been clearly identified, and requires further investigation.

It should also be noted that the delta-of-deltas considered here is rather small, which difficult the task of finding its cause. However, since the trend observed in CFD is consistent with the wind tunnel, it is believed that the observed effect is real, and not due to errors in the simulations.

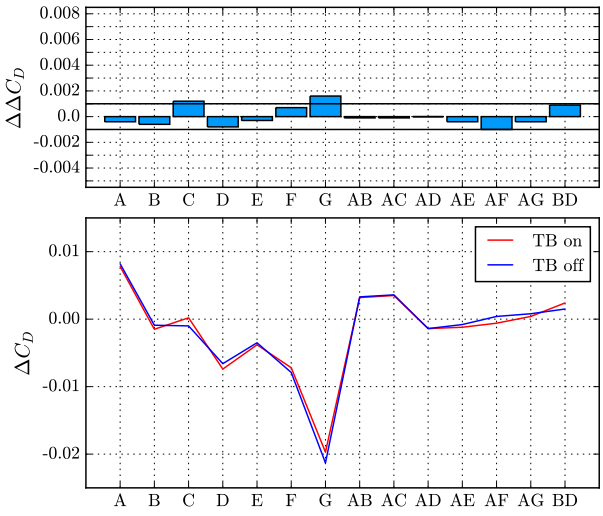

(a) Effects on drag

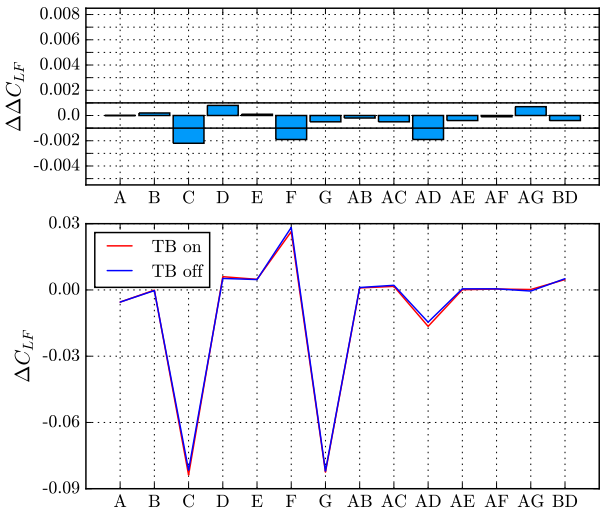

(b) Effects on front lift

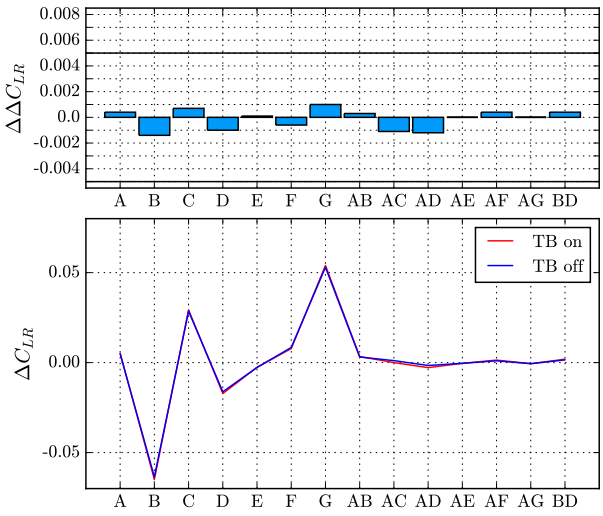

(c) Effects on rear lift

Figure 7: Effects from tangential blowing on force deltas and delta-of-deltas on the notchback. The horizontal black lines in the bar plots indicate the repeatability of the wind tunnel.

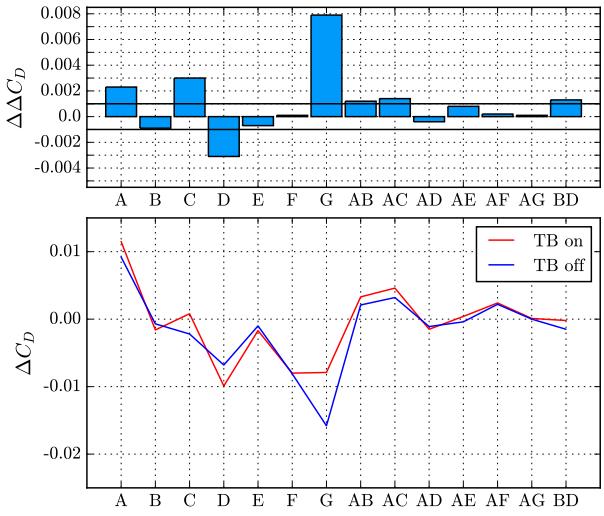

(a) Effects on drag

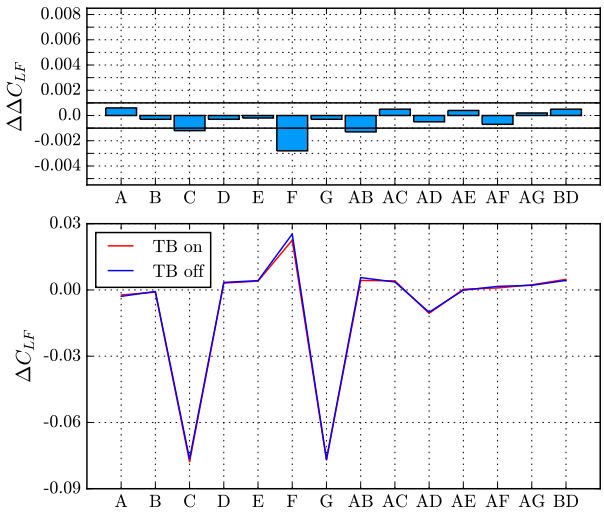

(b) Effects on front lift

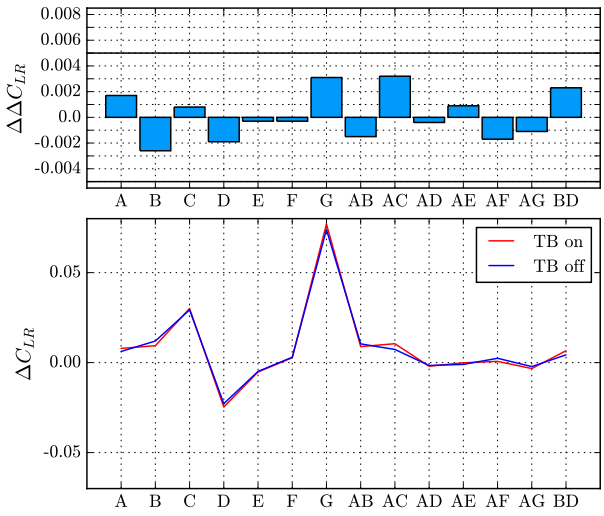

(c) Effects on rear lift

Figure 8: Effects from tangential blowing on force deltas and delta-of-deltas on the squareback. The horizontal black lines in the bar plots indicate the repeatability of the wind tunnel.

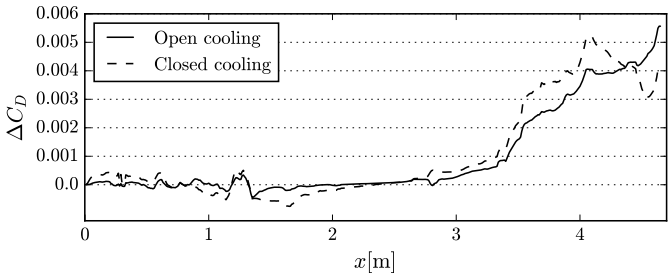

Figure 9: Accumulated drag difference from CFD between blowing on and blowing off over the length of the car.

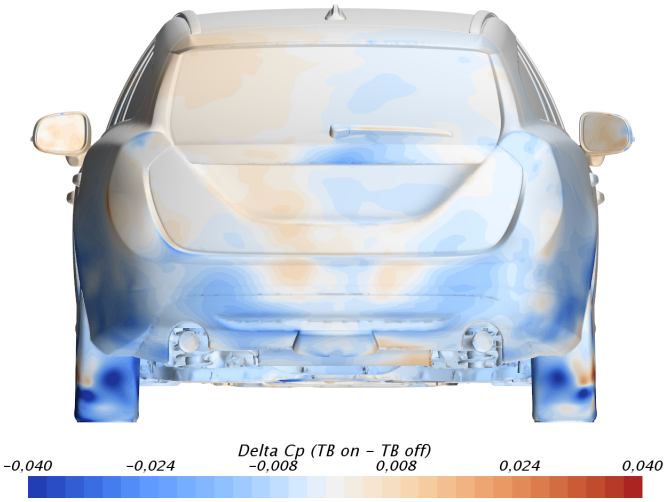

(a) Open cooling

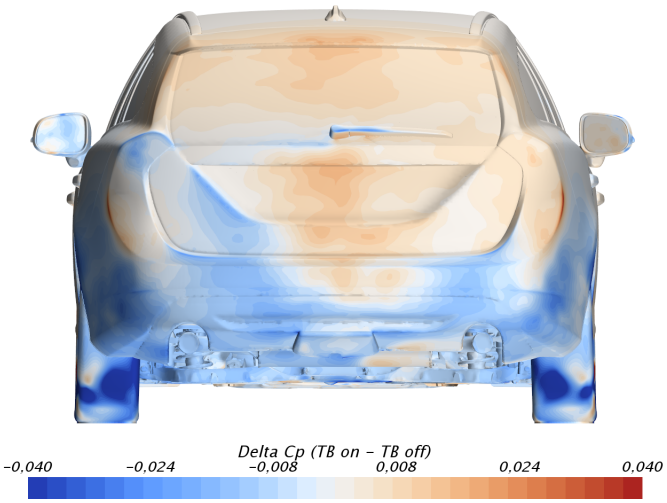

(b) Closed cooling

Figure 10: Difference in pressure coefficient, ΔC_P, on the base of the car.

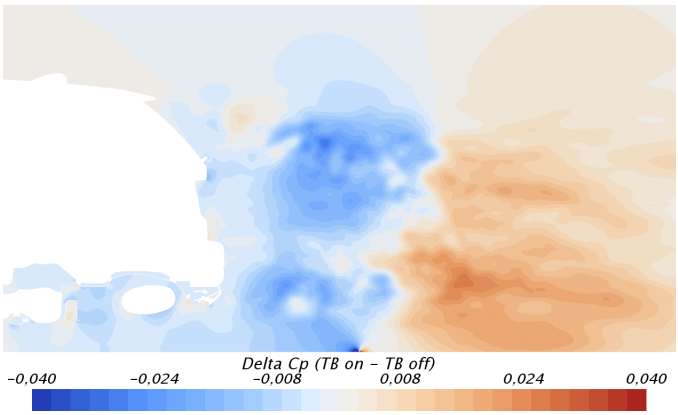

(a) Open cooling

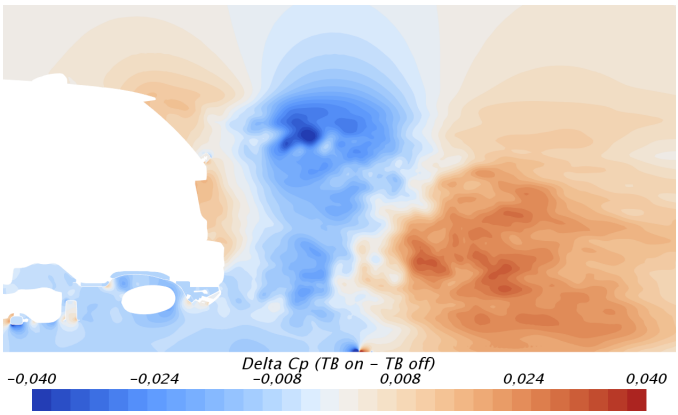

(b) Closed cooling

Figure 11: Difference in pressure coefficient, ΔC_P, on the centre plane of the base wake.

Conclusions

The purpose of this study has been to investigate the effects from aft-belt tangential blowing on the forces measured on two vehicles in the wind tunnel. Based on the results presented, the following conclusions are drawn:

1. For the empty wind tunnel, the displacement thickness of the boundary layer 800 mm behind the tangential blowing slot is reduced by the tangential blowing and even vanishes in some regions along the width of the slot, but shows a large nonuniformity.

2. The main features of the boundary layer thickness behind the blowers can be captured in CFD using a simplified modeling approach. However, none of the observed nonuniformities believed to be caused by the moving belts are seen in the simulations.

3. The squareback with its larger base wake is more sensitive to tangential blowing effects than the notchback, especially for drag.

4. Configurations with a large impact on the underbody flow, such as air dam, underbody panels, ride height and cooling blanking, are most sensitive to tangential blowing.

5. Based on the CFD simulation results for the squareback, it is believed that the main reason for the different sensitivities for the top hats is the changes in the pressure on the upper part of the base area introduced by the tangential blowing.

References

[1] Wiedemann, J., "The Influence of Ground Simulation and Wheel Rotation on Aerodynamic Drag Optimization - Potential for Reducing Fuel Consumption", (Feb. 1, 1996), DOI: 10.4271/960672.

[2] Berndtsson, A., Eckert, W. T., and Mercker, E., "The Effect of Groundplane Boundary Layer Control on Automotive Testing in a wind Tunnel", (Feb. 1, 1988), DOI: 10.4271/880248.

[3] Mercker, E. and Knape, H., "Ground Simulation with Moving Belt and Tangential Blowing for Full-scale Automotive Testing in a wind Tunnel", (Feb. 1, 1989), DOI: 10.4271/890367.

[4] Mercker, E. and Wiedemann, J., "Comparison of Different Ground Simulation Techniques for Use in Automotive Wind Tunnels", *SAE Technical Paper 900321*, (Feb. 1, 1990), DOI: 10.4271/900321.

[5] Cogotti, A., "Ground Effect Simulation for Full-Scale Cars in the Pininfarina Wind Tunnel", *SAE Technical Paper 950996*, (Feb. 1, 1995), DOI: 10.4271/950996.

[6] Potthoff, J., "Future Road Simulation Techniques in the IVK/FKFS Wind Tunnels", *Progress in Vehicle Aerodynamics-Advanced Experimental Techniques* 2, 2000.

[7] Sternéus, J., Walker, T., and Bender, T., "Upgrade of the Volvo Cars Aerodynamic Wind Tunnel", *SAE Technical Paper 2007-01-1043*, (Apr. 16, 2007), DOI: 10.4271/2007-01-1043.

[8] Box, G. E. P., Hunter, J. S., and Hunter, W. G., "Statistics for Experimenters: Design, Innovation and Discovery", 2. ed, Wiley series in probability and statistics, (Hoboken, N.J, Wiley-Interscience, 2005), 633 pp., ISBN: 978-0-471-71813-0.

[9] Olander, M., "CFD Simulation of the Volvo Cars Slotted Walls Wind Tunnel", Masters Thesis, Chalmers University of Technology, 2011.

Contact Information

Emil Ljungskog
Dept. of Applied Mechanics
Chalmers University of Technology
412 96 Göteborg
emil.ljungskog@chalmers.se

Acknowledgements

This work was funded by FFI (*Fordonsstrategisk Forskning och Innovation*, Strategic Vehicle Research and Innovation) through Vinnova (Sweden's innovation agency), and Volvo Cars.